“Converted Wave Noise” and Conventional P-Wave Data

Arnim B. Haase, Geo-X Systems Ltd. and Bill N. Goodway, PanCanadian Petroleum

Introduction

It has long been recognized that vertical geophones detect converted waves to some degree (Ferber, 1990; Claerbout, 1992; Ogilvie and Purnell, 1996; Holmes and Edwards, 2000; Guevara and Cary, 2000).This effect is sometimes referred to as leakage or crosstalk. There are even reports of hydrophones detecting doubly converted waves (Jain, 1988; Bevc et al., 2000). Generally, this converted wave energy on conventional P-wave data is considered noise because it is relatively weak, occurs at larger offsets and is successfully dealt with by conventional multiple attenuation. However sometimes converted waves leak through to the stack and could potentially lead to misinterpretation; in these cases identification of converted wave events is crucial (Ogilvie and Purnell, 1996; Holmes and Edwards, 2000; Bevc et al., 2000). Some authors even indicate the potential of obtaining additional information from this converted wave interference in P-wave data (Ameely et al., 1985; Jain, 1988; Ogilvie and Purnell, 1996; Harilal et al., 1999; Jones and Gaiser, 1999; Bevc et al., 2000).

The purpose of this study is to investigate the extraction of "converted wave noise" from P-wave data recorded in the Western Canadian Sedimentary Basin with the eventual aim of identifying converted wave contamination and possibly estimating the Vp/Vs background.

Modelling of PS-converted waves

The modelling results shown in Figs. 1 and 2 are based on a specific real data example from west-central Saskatchewan. Offset dependent traces are computed from sonic and density logs by invoking the convolutional model and using a minimum phase wavelet. Primary P-wave events with first order P-wave surface multiples as well as primary converted PS-waves are modelled. Reflection amplitudes for primaries and multiples are based on Zoeppritz equations; PS-reflectivity is computed with a linearized approximation to Zoeppritz equations from Aki and Richards (1980). The signal strength of converted waves is derived by assuming point receivers and taking the vertical component of the wavefield emerging at the surface. As log data is unavailable for the first 120m of the subsurface, the velocity and density measured at 120m depth are assigned to this near surface layer. Figs. 1 and 2 are Radon domain displays (velocity scans, Claerbout 1992) where the vertical axis is two-way travel time in milliseconds and the horizontal axis shows velocities in metres per second (increasing from left to right). Contrast is enhanced by decreasing the relative signal strength of P-wave primaries and then squaring of all amplitudes. Fig. 1 is computed for a constant Vp/Vs ratio of 1.5; the ratio for Fig. 2 is 2.5. There is no primary energy beyond about 560ms in these models. In the extreme case of Vp/Vs = 2.5 converted waves are well separated from primaries and multiples. In the other extreme (Vp/Vs = 1.5) there is less separation and there would be more separation problems at larger two-way travel times.

Data example

The modelling study provides information as to where to look for converted wave energy in a velocity scan of real data. Following conventional P-wave processing, gathers are usually dominated by primary energy and velocity scans are overwhelmed by it. Therefore, as a first step for converted wave extraction from conventional P-wave data, the primaries must be attenuated as much as possible. Evidence for converted waves can sometimes be found on semblance displays of common offset stacks (not shown in this abstract), but because of potentially large residual shear statics the better domain for this investigation is the common receiver gather (Garotta, 1999). Fig. 3 shows a contrast enhanced velocity scan of a real data common receiver gather following P-wave processing and primary attenuation. Firstly, despite attenuation, the primaries are still the most energetic events in this display. Secondly, converted wave energy should be expected between 1350m/sec and 1850m/sec (see Figs. 1 and 2) and there is indeed some indication of "converted wave noise". Noise trains above 300ms are considered to be artifacts of the velocity scan. Next, a Radon-filter is employed in order to further attenuate primaries. Then, a non-hyperbolic moveout correction for PS-converted waves is applied to common receiver gathers in a scan of constant Vp/Vs-ratios. Fig. 4 shows such corrected gathers (same receiver as is used for Fig. 3). The panel on the right is computed for Vp/Vs = 1.5 , increasing by 0.1 between panels to Vp/Vs = 2.5 for the panel on the very left. When comparing panels from right to left, some events go from undercorrected on the right to overcorrected on the left. This is exactly how converted waves might be expected to behave. Also note the crossing events between 640ms and 700ms and more interestingly, there are a few events that are still undercorrected in the panel on the left in Fig. 4 at Vp/Vs = 2.5 .

Robert Garotta (1999) describes several mechanisms for conversion near the compressional source location (both vertical vibrators and dynamite charges). These sources can produce significant shear wave energy at angles around 45 degrees to the vertical. If these S-waves are converted to P-waves on reflection then SP-waves should be recorded, which is the reverse of PS-waves. This idea is tested on common shot gathers from the same dataset used above. Fig. 5 shows the velocity scan of such a common shot gather, computations are equivalent to Fig. 3 . When compared to Fig. 3 , there appears to be even more evidence of "converted wave noise" in Fig. 5 . Fig. 6 is the common source equivalent to Fig. 4 (same source as used for the computation of Fig. 5). Again, when comparing panels from right to left, some events go from undercorrected to overcorrected and a few events are still undercorrected at Vp/Vs = 2.5 .

What is the meaning of events undercorrected at Vp/Vs = 2.5 in Figs. 4 and 6 ? Considering the possibility that there could be shear wave conversion at source and that vertical geophones do respond to non-vertical shear waves, these undercorrected events could indicate SS-wave energy. Modelling of SS-waves for the specific data example under investigation shows surprising strength of this mode at far offsets when compared to PS-waves (not shown in this abstract). The SS-model is computed with SS-reflectivity (Aki and Richards, 1980) and assuming the same emergence angle dependent weighting for conversion at source as is used for the vertical geophone. When employing a Radon-filter designed to reject primaries and PS-converted waves, followed by SS-wave moveout correction of common receiver gathers for the range of Vp/Vs from 1.5 to 2.5 , it is found that all suspected SS-wave events are flattened somewhere in this Vp/Vs range (not shown in this abstract).

Conclusions

For the specific data example under investigation there appears to be considerable evidence for converted waves on conventional P-wave data. If proven correct, this could allow the determination of the Vp/Vs-ratio and location of converted wave events on time sections.

What is completely ignored in this investigation is the question of receiver group arrays. For this specific data example, the short group array of 15m helps to reduce array response attenuation. If a geophone array and the shear static surface effects should conspire to completely cancel a non-vertical converted wave arriving from a particular direction, then it is unlikely that a converted wave from the opposite direction is also cancelled. Thus, at least some converted energy will get through.

The computer experiments described above are evidence, but not proof, that converted wave energy has actually been isolated from conventional P-wave data. Proof can only be provided by processing a true multi-component comparison data set, which is intended to be the next step in this ongoing project.

References

Aki, K.T., and Richards, P.G., 1980, Quantitative Seismology: Theory and Methods: Vol. 1, W.H. Freeman and Co.

Ameely, L., Edelmann, H.A.K., and Fertig, J., 1985, How do shear wave events Affect normal P-wave records?: Geophys. Prosp., 33, 201-211.

Bevc, D., Pereyra, V., and Popovici, A.M., 2000, Converted energy in towed-cable and OBC data: 2000 SEG/EAGE Summer Research Workshop Abstracts.

Claerbout, J.F., 1992, Earth Soundings Analysis: Processing versus Inversion: Blackwell Scientific Publications.

Ferber, R.G., 1990, On the design of 2-D convolution filters for separation of P- and S-waves: 60th Ann. Internat. Mtg., Soc. Expl. Geophys., Expanded Abstracts, 1101-1103.

Garotta, R., 1999, Shear waves from acquisition to interpretation: 2000 Distinguished Instructor Short Course, Distinguished Instructor Series, No. 3, Society of Exploration Geophysicists.

Guevara, S.E., and Cary, P.W., 2000, A method for P-P and P-S mode separation in the presence of statics: 70th Ann. Internat. Mtg., Soc. Expl. Geophys., Expanded Abstracts, 1225-1228.

Harilal, S.G., Sharma, N.C., Mishra, S., and Ram, A., 1999, Mode converted shear waves on P-wave data - simulation with numerical modelling: 61st Ann. EAGE Conference, Expanded Abstracts, paper 4-26.

Holmes, G.M., and Edwards, T.K., 2000, Converted waves from coals cannot be ignored: 70th Ann. Internat. Mtg., Soc. Expl. Geophys., Expanded Abstracts, 2017-2019.

Jain, S., 1988, S-wave velocity and Poisson's ratio from shear waves observed in normal P-wave data in an offshore basin: Canadian Journal of Exploration Geophysics, 24, 32-47.

Jones, N., and Gaiser, J., 1999, Imaging beneath high-velocity layers: 69th Ann. Internat. Mtg., Soc. Expl. Geophys., Expanded Abstracts, 713-716.

Ogilvie, J.S., and Purnell, G.W., 1996, Effects of salt-related mode conversions on subsalt prospecting: Geophysics, 61, 331-348.

Acknowledgements

Special thanks to Founders Energy for providing the data example.

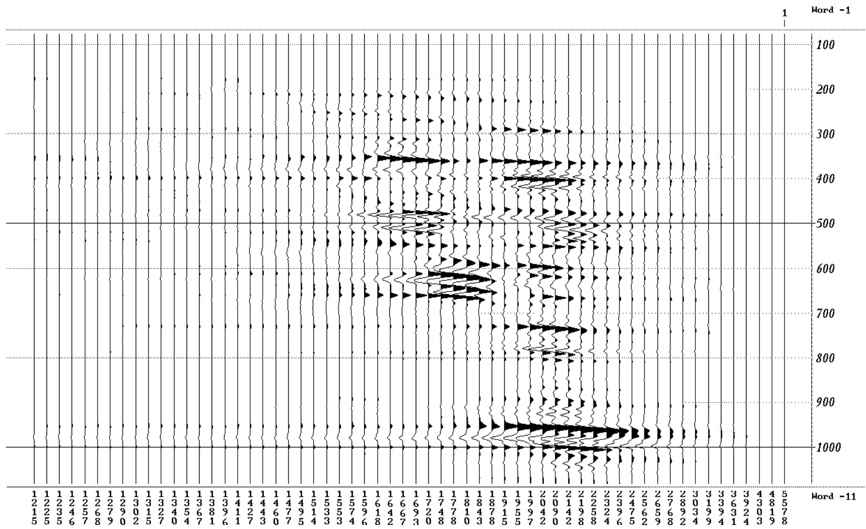

Fig. 1: Velocity scan of model at V_P/V_S=1.5

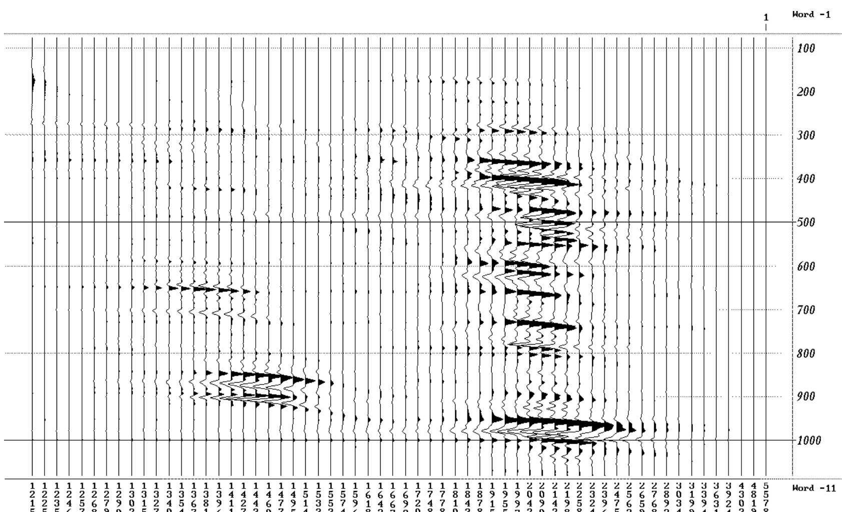

Fig. 2: Velocity scan of model at V_P/V_S=2.5

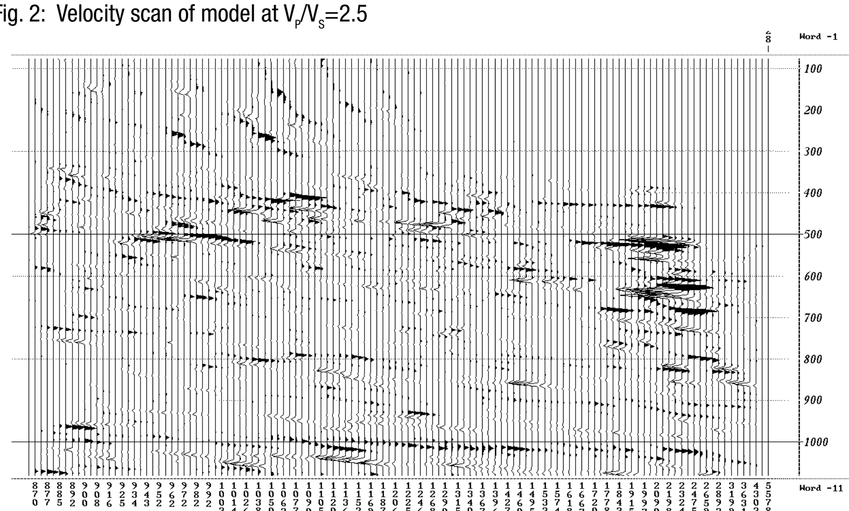

Fig. 3: Velocity scan of common receiver gather

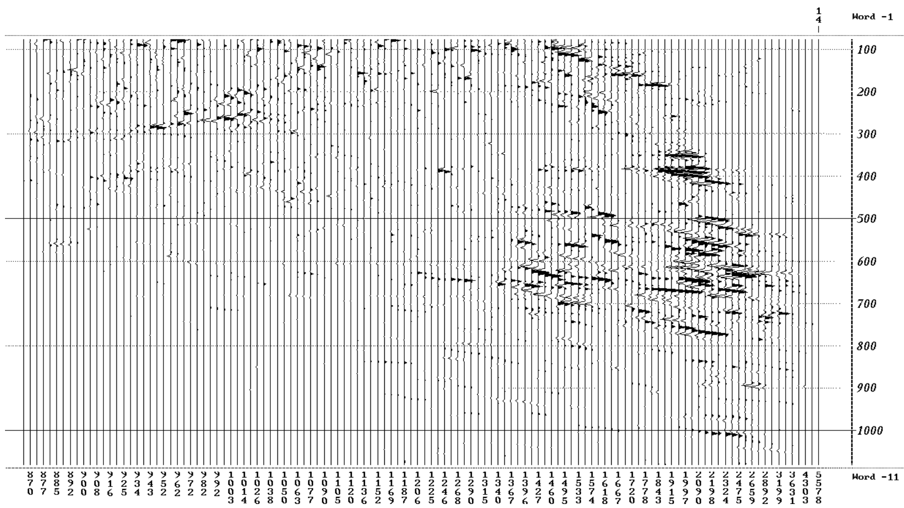

Fig. 4: NMO corrected common receiver gather panels

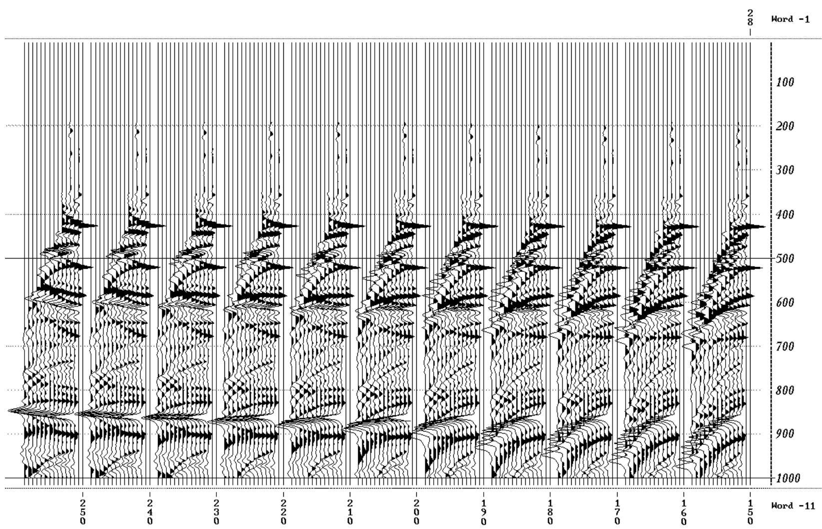

Fig. 5: Velocity scan of common source gather

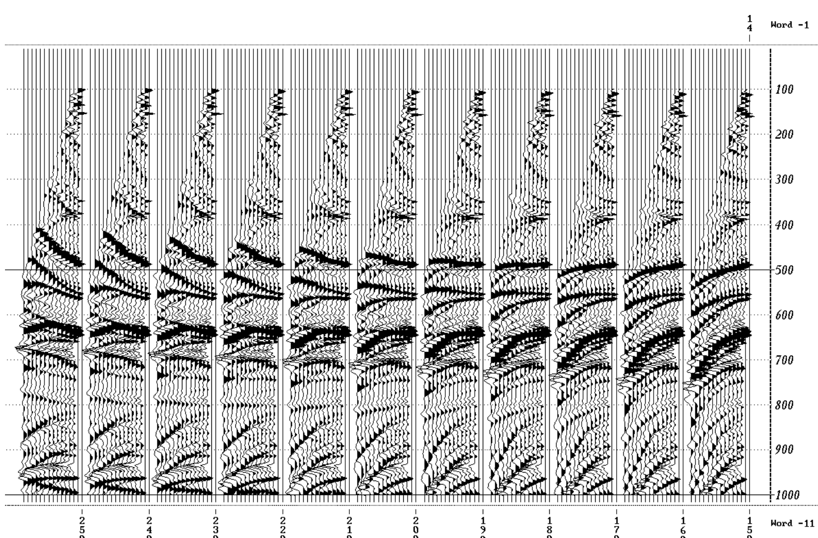

Fig. 6: NMO corrected common source gather panels